



Design and phase transition behavior of siloxane-based monomeric and dimeric liquid crystals bearing cholesteryl mesogenic groups

Kaito Katsuki^a, Kosuke Kaneko^{a, b, *}, Kimiyoshi Kaneko^a, Riki Kato^b, Nobuyoshi Miyamoto^b, Tomonori Hanasaki^a

^a Department of Applied Chemistry, College of Life Sciences, Ritsumeikan University, 1-1-1 Nojihigashi, Kusatsu, Shiga, 525-8577, Japan

^b Department of Life, Environment, and Applied Chemistry, Faculty of Engineering, Fukuoka Institute of Technology, 3-30-1 Wajiro-higashi, Higashi-ku, Fukuoka, 811-0295, Japan

ARTICLE INFO

Article history:

Received 26 December 2018

Received in revised form

14 February 2019

Accepted 18 February 2019

Available online 20 February 2019

Keywords:

Liquid crystal

Siloxane

Cholesteryl group

Blue phase

ABSTRACT

A series of siloxane-based monomeric and dimeric liquid crystals (LCs) bearing cholesteryl mesogenic groups were newly synthesized and their phase transition behavior was investigated by polarized optical microscopy (POM), differential scanning calorimetry (DSC), and X-ray diffraction (XRD). All the siloxane-based LCs obtained in this study showed a smectic A phase in a wide temperature range. Among the siloxane-based LCs obtained, only the dimeric LC with a shortest siloxane unit at a central part of a spacer was found to exhibit a chiral nematic phase and a blue phase in addition to the smectic A phase. The difference in the thermal properties of the siloxane-based dimeric LCs was investigated in terms of their conformations. Furthermore, the results obtained for the siloxane-based LCs were discussed with comparing with those of homologues having the normal alkyl chains and spacers.

© 2019 Elsevier B.V. All rights reserved.

1. Introduction

Self-assembly in molecular science is one of the outstanding tools for fabricating functional nanomaterials. Highly ordered architectures in the nanostructured materials are fundamental factors dictating unique features in molecular biology, chemistry, polymer science, materials science, and engineering [1]. Such molecular self-assembly systems accelerate a significant advance in modern scientific technology, and are attracting a great deal of attention. Over the past few decades, the self-assembly of liquid crystals (LCs) responsive to external environments, has proven to be a very useful tool creating the well-ordered materials [2]. Depending on the chemical structure and molecular shape, a variety of LC phases can be formed, and furthermore their structures are changeable by external stimuli for example electric/magnetic field, light, temperature, and mechanical forces. For the construction of the nanostructured materials using the LCs, hybrid organic/inorganic molecules such as those based on siloxane moieties are attractive and feasible. The chemical immiscibility of the organic

and inorganic parts leads to nanosegregation into highly ordered nanostructures [3].

There has been an increasing interest in LC dimers consisting of two mesogenic groups connected by a flexible spacer, due to their interesting phase behavior which significantly differs from that of the corresponding monomeric LCs. Since LC dimers were firstly reported by Vorländer in 1927 [4], symmetrical dimers composed of two structurally identical mesogenic groups linked through a flexible central spacer such as a polymethylene group have been widely investigated, especially during the past two decades [5]. The transition properties of the LC dimers are strongly dependent on the nature and length of the flexible spacer [6]. For example, an odd-even effect for the clearing and melting points has been observed by changing the length of the spacer between the two mesogenic groups. In addition, the design of twist bend nematic (N_{tb}) phases arising from the LC dimers is a very hot topic in the molecular science of the LCs recently [7]. From the scientific background mentioned above, the study of such unique phase properties in the LC dimers is still an important subject. Presently, a standard approach for understanding of the properties is to investigate stabilities of two identical mesogenic groups (symmetrical dimers) [8], unsymmetrical instabilities (unsymmetrical dimers) [9], innate mesogenic properties depending on its molecular structure [8], length and flexibilities of spacers [8], connection

* Corresponding author. Department of Applied Chemistry, College of Life Sciences, Ritsumeikan University, 1-1-1 Nojihigashi, Kusatsu, Shiga, 525-8577, Japan.
E-mail address: kaneko@fc.ritsumei.ac.jp (K. Kaneko).

mode between mesogenic groups and spacers (terminally, vertically) [10], and conformations of overall molecule (linear, tilt, bent) [11].

The present study is focused on the siloxane-based monomeric and dimeric LCs bearing cholesteryl mesogenic groups, which could be categorized as hybrid organic/inorganic LC dimers, and their phase transition behavior was characterized by polarising optical microscopy (POM), differential scanning calorimetry (DSC) and X-ray diffraction (XRD). The incorporation of the siloxane unit into the spacers for the dimeric LCs is an essential scientific topic for studying the molecular design of the LC materials with the unique properties deriving from its flexibility and nanosegregation. We investigated also how the siloxane unit in the spacer and tail influences on the thermal properties of the homologues having the normal alkyl chains and spacers. The synthetic scheme of the siloxane-based LCs is presented in Fig. 1.

2. Experimental

2.1. Materials

The reagents, allyl bromide, methyl 4-hydroxybenzoate, cholesterol, 1,1,1,3,3-pentamethyldisiloxane, 1,1,1,3,3,5,5-heptamethyltrisiloxane, 1,1,3,3-tetramethyldisiloxane, 1,1,3,3,5,5-hexamethyltrisiloxane, 1,1,3,3,5,5,7,7-octamethyltetrasiloxane, and the organic solvents, 2-butanone, methanol, dichloromethane, toluene were purchased from Tokyo Chemical Industry Co., Ltd. 1-Ethyl-3-(3-dimethylaminopropyl)-carbodiimide (EDC) and *N,N*-dimethyl-4-aminopyridine (DMAP) were purchased from FUJIFILM Wako Pure Chemical Corporation. Potassium carbonate was

purchased from Nacalai Tesque, Inc. Toluene was dried over sodium and then distilled, and other solvents were used without further purification. Synthetic routes of the objective siloxane-based LCs are shown in Fig. S1.

2.2. Characterization

Thermal properties were measured using a Diamond DSC (Perkin-Elmer, Inc. MA, USA) at heating and cooling rates of $5\text{ }^{\circ}\text{C min}^{-1}$. The optical textures of the liquid crystalline phases were observed on a Nikon ECLIPSE LV100 polarising optical microscope (POM) equipped with Mettler-Toledo FP-82HT hot-stage and FP-90 central processor. ^1H NMR spectra were recorded on an ECS 400 NMR spectrometer (JEOL Ltd., Tokyo, Japan) at 400 MHz, using CDCl_3 as the solvent. Chemical shifts (δ) are expressed in ppm relative to tetramethylsilane (TMS, $\delta = 0.0$ ppm) as internal standard for **A**, **B** and **C**, or from the residual chloroform signal (CHCl_3 , $\delta = 7.24$ ppm) for **D-*n***, ($n = 2, 3$) and **E-*n*** ($n = 2, 3, 4$). The alignment of the LCs was checked on the POM observation by using the non-treated glass cells (E.H.C. Co. Ltd, Japan). Structural analyses by SAXS were performed with the Rigaku NANOPIX (Cu $K\alpha$ radiation at 30 V and 40 mA) with a camera distance of 220 mm. For SAXS measurements, the samples were introduced into a thin glass capillary with a thickness of 1.5 mm.

3. Results and discussion

The phase transition behavior of the siloxane-based LCs obtained in this study is discussed in the following two sections: (1) the thermal behavior of the monomeric LCs (**D-*n***, $n = 2, 3$) and

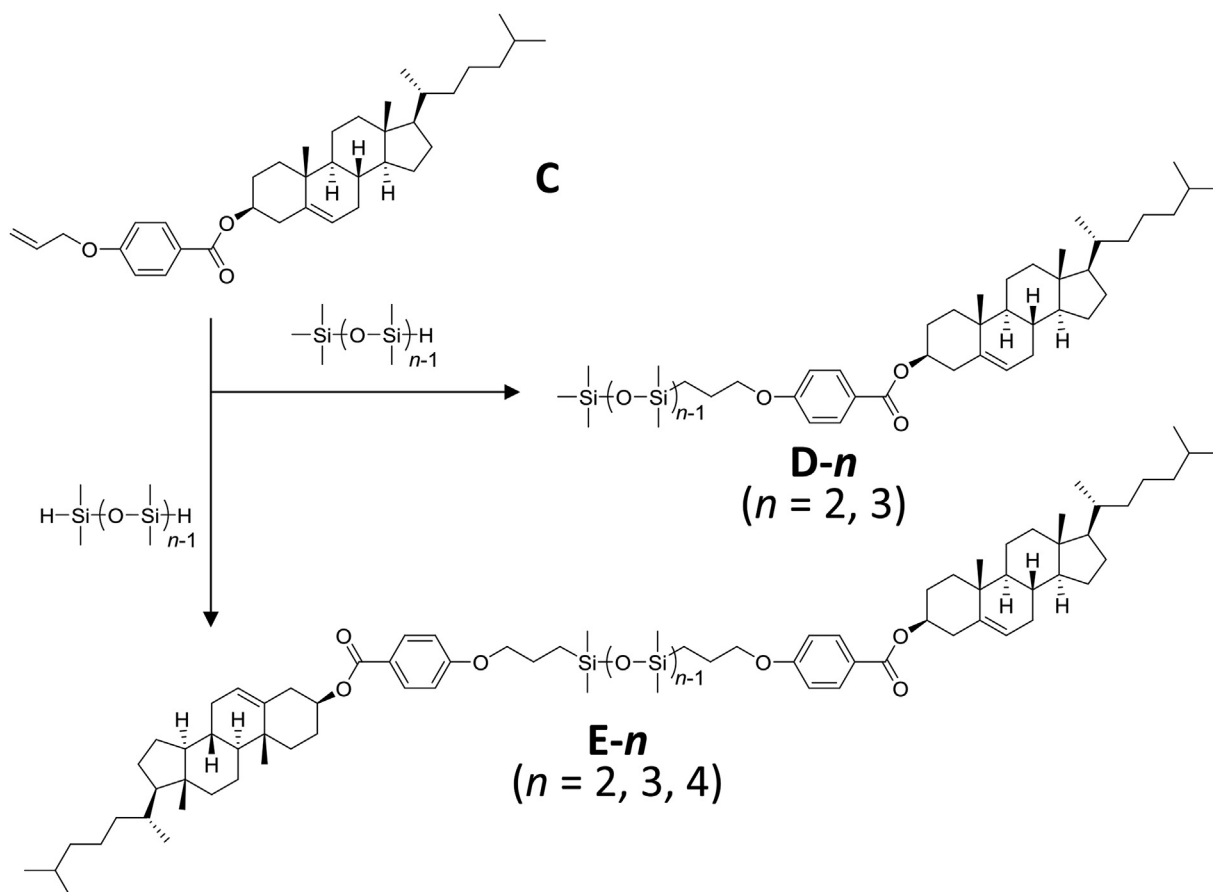


Fig. 1. Synthetic scheme of the siloxane-based LCs bearing the cholesteryl mesogenic groups.

dimeric ones (**E-n**, $n = 2, 3, 4$), and (2) the influence of the siloxane units on the thermal behavior of the corresponding LC materials having normal alkyl chains. The thermal properties of all the siloxane-based LCs summarized in Table S1 were studied by differential scanning calorimetry (DSC), polarising optical microscopy (POM) and X-ray diffraction (XRD) analysis.

3.1. Monomeric (**D-n**) and dimeric (**E-n**) siloxane-based LCs

First of all, the compound **C** which is a precursor of all the siloxane-based LCs was found to show a chiral nematic (N^*) phase in a temperature range from 124 °C to 226 °C [12]. The POM images, DSC chart and XRD profile of **D-2** are shown in Fig. 2. On the POM observations, **D-2** exhibited a focal conic texture typical of a smectic A (SmA) phase. In the DSC diagram on heating, the endothermic peak was detected at 110.0 °C. This temperature is in good agreement with the temperature at which the focal conic texture appeared in the POM studies. On the further heating, the endothermic peak at 161.2 °C corresponds to a clearing point with the disappearance of the texture in the POM image. The small-angle XRD pattern for **D-2** at 150.0 °C shows a sharp peak in the small angle region ($2\theta = 2.53^\circ$, $d = 34.9 \text{ \AA}$) and a broad peak in the wide angle region ($2\theta = 16.0^\circ$, $d = 5.5 \text{ \AA}$) corresponding to the lateral spacing between the rod-like molecules. The focal conic structure observed in the POM image and the characteristic XRD pattern with a very sharp reflection and a diffuse reflection of the alkyl tails were indicative of the formation of the SmA phase.

According to the molecular modelling calculation in the extended conformation using ChemBio3D-Ultra, employing MM2 minimal energy, the estimated molecular length (L) of the most extended conformation is about 34.5 Å. As a result, a calculated d/L ratio is about 1.0 ($L \approx d$), suggesting that the LC molecules are packed in a single smectic layer as demonstrated in Fig. 3. The hybridization of immiscible organic and inorganic components in the molecular construction at the nanoscale generally leads to nanosegregation, and the each site tends to gather separately. Therefore, such molecular design in **D-2** provides the nanosegregated LC organization formed by the siloxane domains and the ones consisting of the alkyl chains and the cholesteryl mesogenic groups, resulting in the stable SmA phase.

The trend in the phase behavior for **D-3** was similar to that for **D-2** (Figs. S2–S5). The length of the siloxane unit is a key factor

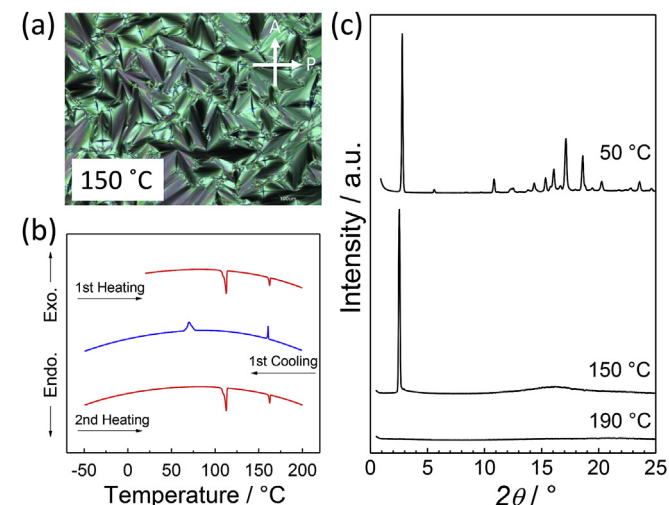


Fig. 2. (a) POM image at 150 °C on heating, (b) DSC chart and (c) XRD profiles recorded at 50 °C (Cryst.), 150 °C (SmA), and 190 °C (Iso.) for **D-2**.

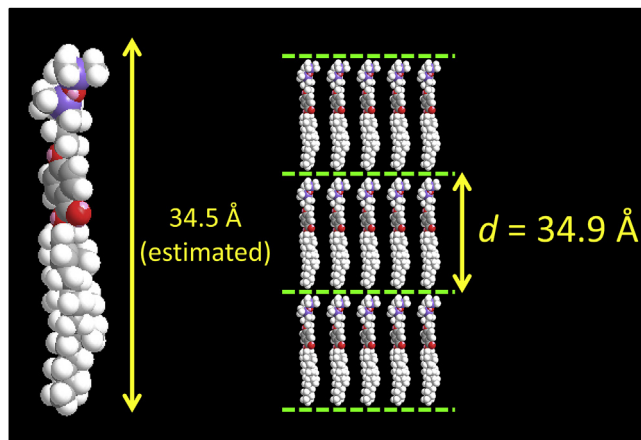


Fig. 3. Illustration of the possible molecular packing of **D-2** in the SmA phase.

determining the mesophase stability. **D-3** with the longer siloxane unit possesses the wider LC temperature range, providing not only the lowered clearing point but also the significant decrease in its melting point. It is reasonable to conclude that the flexibility of the siloxane unit suppressed its crystallization. The XRD profile of **D-3** demonstrated a typical characteristic of the SmA phase, and its d -spacing (39.4 Å) is longer than that of **D-2**. The difference in the d -spacing is due to the addition of the siloxane unit (the bond distance of Si–O is 1.64 Å, and the Si–O–Si angle is 142.5° [13]).

The drastic change of the phase behavior for **D-n** ($n = 2, 3$) was demonstrated by the simple modification of the chemical structures in comparison of that of the compound **C**. The addition of the siloxane unit resulted in the remarkable decrease in the clearing point and also the suppression of the crystallization. Furthermore, the SmA phases were induced by the addition of the siloxane unit.

The phase transition behavior for the dimeric series **E-n** ($n = 2, 3, 4$) is described here. With regard to the dimeric siloxane-based LCs, the interesting phase behavior was unexpectedly observed depending on the number of the siloxane unit connected in a central part of the spacer. The POM images, DSC chart and XRD profile for **E-2** are shown in Fig. 4. The dimeric LC (**E-2**) with a shortest siloxane central unit showed the enantiotropic smectic A phase, N^* phase, and blue phase (BP), which were characterized on the basis of the POM textures. The DSC chart displayed the three endothermic peaks on heating. The melting point of **E-2** is 140.0 °C, whereas its clearing point is 226.1 °C. These results revealed that the respective transition temperatures are higher than these of **D-n** ($n = 2, 3$). The platelet texture of the BP was observed only upon scanning with the rate of $2.0 \text{ }^\circ\text{C min}^{-1}$ on the POM observation. In the XRD profile for **E-2** at 180.0 °C shown in Fig. 4, a sharp peak in the small angle region ($2\theta = 2.80^\circ$, $d = 31.5 \text{ \AA}$) and a broad peak in the wide angle region ($2\theta = 16.0^\circ$, $d = 5.5 \text{ \AA}$) were detected. The half length of the full stretched molecular structure of **E-2** is calculated to be about 31.2 Å, consequently suggesting a U-shaped conformation of the dimer packed in the smectic layers [14], as illustrated in Fig. 5.

In contrast to **E-2**, only smectic A phase was observed for **E-3** and **E-4** (Figs. S2–S4). They showed the slight decrease in their clearing points but the gradually lowered melting points as increasing the number of the siloxane units. As a result, the wider LC temperature range was obtained, where ΔT (LC range) was 86 °C for **E-2**, 128 °C for **E-3**, and 160 °C for **E-4**, respectively as shown in Fig. 6. The change of the melting points for **E-n** ($n = 2, 3, 4$) is resulted from the additional flexibility of the siloxane units and its associated suppression of the crystallization, which was also

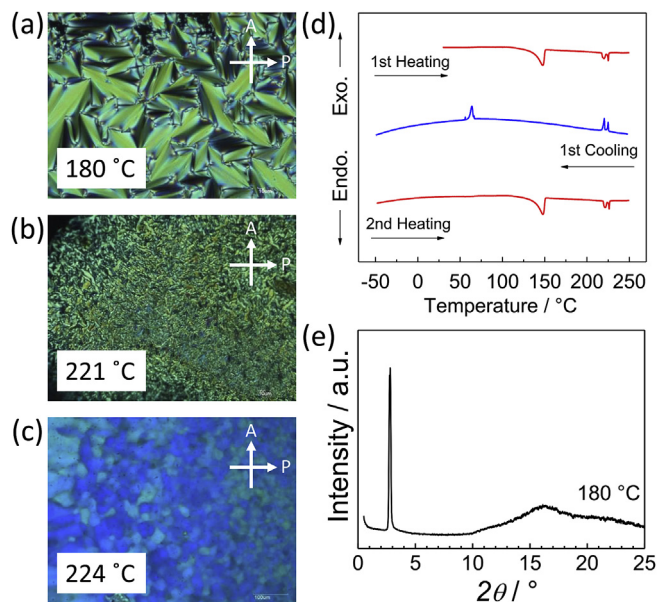


Fig. 4. (a–c) POM images taken on heating, (d) DSC chart and (e) XRD profile for **E-2**. The scanning rate on the POM investigation was (a, b) 5°C min^{-1} and (c) 2°C min^{-1} .

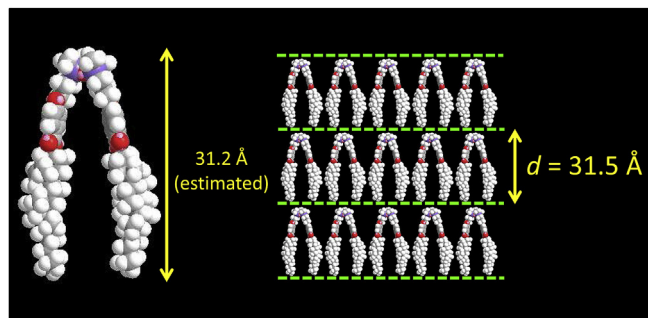


Fig. 5. Illustration of the possible molecular packing of **E-2** in the SmA phase.

observed for **D-*n*** ($n = 2, 3$).

The XRD profiles in a small angle region ($2\theta = 0\text{--}10^\circ$) obtained for **D-*n*** ($n = 2, 3$) and **E-*n*** ($n = 2, 3, 4$) are displayed in Fig. 7. The respective data were recorded in their smectic A phases. As mentioned earlier, the d -spacings of **D-2** and **D-3** were 34.9 Å and 39.4 Å, respectively, and the difference of the d -spacing is attributed to the one siloxane unit. On the other hand, from the profiles of **E-*n*** ($n = 2, 3, 4$), it is apparent that the shift of the d -spacing corresponding the smectic layers is smaller in comparison with **D-*n*** ($n = 2, 3$). This different trend can be explained by considering the conformations of **D-*n*** ($n = 2, 3$) and **E-*n*** ($n = 2, 3, 4$). The rod-shaped molecules of **D-*n*** ($n = 2, 3$) are perpendicularly oriented in the smectic layers. The siloxane unit was connected at the terminal part of the molecule, thereby the addition of the siloxane unit directly affected the difference in the d -spacing. In contrast, the siloxane unit was introduced at the central part of the spacer for **E-*n*** ($n = 2, 3, 4$). As illustrated in Figs. 5, S6, and S7, we proposed the U-shaped conformations of **E-*n*** ($n = 2, 3, 4$) in the smectic layers on the basis of the d -spacing obtained. Because of this conformation, the increase of the siloxane unit had a small impact on the d -spacing for **E-*n*** ($n = 2, 3, 4$). Simultaneously, the proposed U-shaped conformations were also supported by the small shift of the d -spacing obtained by the XRD analysis. Furthermore, the longer siloxane unit provides the dimeric molecules wider space enough to form the U-shaped conformations. This could be linked to the appearance of the stable smectic A phase for **E-3** and **E-4**. By contrast, the N^* phase and the BP were observed for **E-2** by the insufficient length and space at the central part, which could be related to the incomplete ordering (like V-shaped) between the mesogenic groups within the molecule.

3.2. Influence of the siloxane units on the thermal properties

Finally, we discuss the influence of the siloxane units on the thermal properties of the homologues having the normal alkyl chains reported in the literature. The N^* phase was observed for all the monomeric homologues having the normal alkyl chain ($n = 1\text{--}12$) [15], and an odd-even effect was apparent in its clearing temperatures. The monomeric homologues having the long alkyl chain ($n \geq 7$) showed the smectic phases with the wider

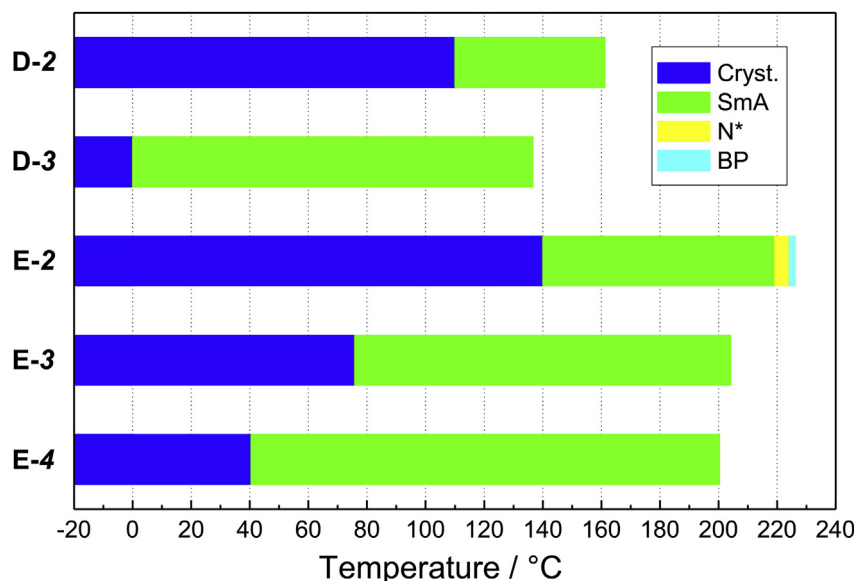


Fig. 6. Phase transition behavior of the siloxane-based monomeric (**D-*n***; $n = 2, 3$) and dimeric LCs (**E-*n***; $n = 2, 3, 4$).

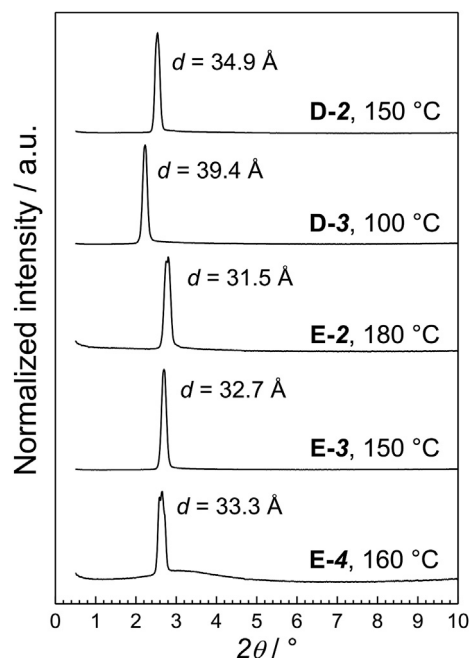


Fig. 7. XRD profiles in a small angle region ($2\theta = 0\text{--}10^\circ$) in the SmA phases obtained for **D-*n*** ($n = 2, 3$) and **E-*n*** ($n = 2, 3, 4$).

temperature range as a function of the number of the carbon atoms. The homologues having the alkyl chain ($n = 7, 9$) showed the phase sequences; Cryst. 129 Sm 138 N* 210 Iso. ($n = 7$) and Cryst. 139 Sm 166 N* 194 Iso. ($n = 9$), of which the tail length is comparable as **D-*n*** ($n = 2, 3$), respectively. As mentioned above, **D-*n*** ($n = 2, 3$) showed only the SmA phase, and the notable difference in the phase behavior is that the N* phase disappeared for **D-*n*** ($n = 2, 3$) and the considerably decrease in the melting points and clearing points was observed. This was due to a stabilization of the SmA phase probably by a nanosegregation of the incompatible siloxane unit [16].

On the other hand, the dimeric LCs having the normal alkyl spacers ($n = 4\text{--}12$) had been found to show the N* phase in a temperature range over 200 °C and the odd-even effect in both the clearing points and melting points [17]. It is common that LC dimers exhibit a remarkable odd-even effect of the transition temperatures, and the behavior has been generally explained on the basis of the molecular shapes of the *all trans*-conformation of the dimers depending on the odd- and even-membered spacers. The dimeric LCs having the normal alkyl spacers ($n = 9, 11$) showed the phase sequences; Cryst. 210 N* 265 Iso. ($n = 9$) and Cryst. 193 N* 260 Iso. ($n = 11$) [17], of which the spacer length is comparable as **E-*n*** ($n = 2, 3$), respectively. (There have been no reports about the LC dimer with the alkyl chain length comparable to that of **E-4**). The introduction of the siloxane unit in the spacer of the dimeric LCs resulted in the pronounced enlargement of the LC temperature range and induced the SmA phase for **E-*n*** ($n = 2, 3, 4$) and a narrow range of the BP only for **E-2**. The apparent difference in the phase transition behavior is the emergence of the SmA phases by the introduction of the siloxane unit. Such higher SmA stability seen for **E-*n*** ($n = 3, 4$) is presumably attributed to a close interaction between the mesogenic groups within the molecule, that would be enhanced by the U-shaped conformation accompanying with the longer siloxane unit in the spacer. Furthermore, the emergence of the BP was interestingly obtained only for **E-2**. This is attributed to that the length of the central siloxane moiety in the spacer of **E-2** is insufficient enough to form the stable U-shaped conformations in the SmA phase. The origin of the BPs for LC dimers has been widely

discussed from a view point of the conformation [18]. At the higher temperature range above the SmA phase, **E-2** might form the bent conformation because of the unstable U-shaped conformation.

4. Conclusion

Identical types of the siloxane-based monomeric and dimeric LCs bearing the cholesteryl mesogenic groups have been synthesized and characterized. The mesomorphic behavior was found to be greatly governed by the modification using the siloxane units in comparison of those of the corresponding LCs having the normal alkyl chains and spacers. Furthermore, the nature of the LC phases was associated with the nanosegregation of the constituent parts of the molecules consisting of the cholesteryl mesogenic groups, the alkyl chains and the siloxane unit. For all the siloxane-based LCs obtained in this study, the SmA phases were induced by the contribution of the siloxane units in compared with those of the homologues having the normal alkyl spacers and tails. Especially, the dimeric LC (**E-2**) with a shortest siloxane central unit showed interestingly the BP in addition to the SmA and the N* phase. This precise study provided some useful insights into the molecular design of hybrid organic/inorganic LCs towards variety of nature of LC phases.

Acknowledgment

This work was partially supported by MEXT-supported Program for the Strategic Research Foundation at Private Universities (2012–2016). We thank Mr. Yuta Kitajima (Ritsumeikan University) for technical assistance with the experiments and fruitful discussions.

Appendix A. Supplementary data

Supplementary data to this article can be found online at <https://doi.org/10.1016/j.jorgchem.2019.02.016>.

References

- [1] (a) N. Giuseppone, *Acc. Chem. Res.* 45 (2012) 2178–2188; (b) E. Busserson, Y. Ruff, E. Moulin, N. Giuseppone, *Nanoscale* 5 (2013) 7098–7140.
- [2] (a) J. Uchida, M. Yoshio, S. Sato, H. Yokoyama, M. Fujita, T. Kato, *Angew. Chem. Int. Ed.* 56 (2017) 14085–14089; (b) T. Kato, J. Uchida, T. Ichikawa, T. Sakamoto, *Angew. Chem. Int. Ed.* 57 (2018) 4355–4371; (c) L. Wang, A.M. Urbas, Q. Li, *Adv. Mater.* (2018), 1801335.
- [3] (a) N. Kim, D.Y. Kim, M. Park, Y.J. Choi, S. Kim, S.H. Lee, K.U. Jeong, *J. Phys. Chem. C* 119 (2015) 766–774; (b) K. Nickmans, J.N. Murphy, B. Waal, P. Leclère, J. Doise, R. Gronheid, D.J. Broer, A.P.H.J. Schenning, *Adv. Mater.* 28 (2016) 10068–10072; (c) J.A. Berrocal, R.H. Zha, B.F.M. de Waal, J.A.M. Lugger, M. Lutz, E.W. Meijer, *ACS Nano* 11 (2017) 3733–3741; (d) J.A. Berrocal, J. Teyssandier, O.J.G.M. Goor, S.D. Feyter, E.W. Meijer, *Chem. Mater.* 30 (2018) 3372–3378; (e) W. Wei, H. Xiong, *Langmuir* 34 (2018) 15455–15461.
- [4] D.Z. Vorländer, *Phys. Chem.* 126 (1927) 449–472.
- [5] (a) C.T. Imrie, P.A. Henderson, *Curr. Opin. Colloid Interface Sci.* 7 (2002) 298–311; (b) C.T. Imrie, P.A. Henderson, *Chem. Soc. Rev.* 36 (2007) 2096–2124; (c) G.Y. Yeap, T.C. Hng, S.Y. Yeap, E. Gorecka, M.M. Ito, K. Ueno, M. Okamoto, W.A.K. Mahmood, C.T. Imrie, *Liq. Cryst.* 36 (2009) 1431–1441; (d) T. Donaldson, H. Staesche, Z.B. Lu, P.A. Henderson, M.F. Achard, C.T. Imrie, *Liq. Cryst.* 37 (2010) 1097–1110.
- [6] (a) P.A. Henderson, A.G. Cook, C.T. Imrie, *Liq. Cryst.* 31 (2004) 1427–1434; (b) P.A. Henderson, J.M. Seddon, C.T. Imrie, *Liq. Cryst.* 32 (2005) 1499–1513; (c) G.R. Luckhurst, *Liq. Cryst.* 32 (2005) 1335–1364.
- [7] (a) V.P. Panov, M. Nagaraj, J.K. Vij, Panarin, Y.P.A. Kohlmeier, M.G. Tamba, R.A. Lewis, G.H. Mehl, *Phys. Rev. Lett.* 105 (2010) 167801; (b) P.A. Henderson, C.T. Imrie, *Liq. Cryst.* 38 (2011) 1407–1414; (c) M. Cestari, S. Diez-Berart, D.A. Dunmur, A. Ferrarini, M.R. de la Fuente, D.J.B. Jackson, D.O. Lopez, G.R. Luckhurst, M.A. Perez-Jubindo, R.M. Richardson, J. Salud, B.A. Timimi, H. Zimmermann, *Phys. Rev. E: Stat., Nonlinear, Soft*

- Matter Phys. 84 (2011), 031704;
(d) R.J. Mandle, *Soft Matter* 12 (2016) 7883–7901;
(e) R.J. Mandle, J.W. Goodby, *Chem. Eur J.* 22 (2016) 18456–18464;
(f) E.E. Pocock, R.J. Mandle, J.W. Goodby, *Soft Matter* 14 (2018) 2508–2514.
- [8] C.T. Imrie, P.A. Henderson, *Chem. Soc. Rev.* 36 (2007) 2096–2124 (and references cited therein).
- [9] (a) C.T. Imrie, *Liq. Cryst.* 33 (2006) 1449–1485;
(b) C.V. Yelamaggad, N.L. Bonde, A.S. Achalkumar, D.S.S. Rao, S.K. Prasad, A.K. Prajapati, *Chem. Mater.* 19 (2007) 2463–2472;
(c) T.N. Chan, Z. Lu, W.S. Yam, G.Y. Yeap, C.T. Imrie, *Liq. Cryst.* 39 (2012) 393–402;
(d) G.Y. Yeap, F. Osman, C.T. Imrie, *Liq. Cryst.* 42 (2015) 543–554.
- [10] (a) A.C. Griffin, S.F. Thames, M.S. Bonner, *Mol. Cryst. Liq. Cryst.* 34 (1976) 135–139;
(b) A.C. Griffin, N.W. Buckley, W.E. Hughes, D.L. Wertz, *Mol. Cryst. Liq. Cryst.* 64 (1981) 139–144;
(c) J. Andersch, C. Tschierske, *Liq. Cryst.* 21 (1996) 51–63;
(d) M. Koipaczyńska, K. Madrak, J. Mieczkowski, E. Górecka, D. Pocięcha, *Liq. Cryst.* 38 (2011) 149–154;
(e) M.C. Varia, S. Kumar, A.K. Prajapati, *Liq. Cryst.* 39 (2012) 365–371;
(f) A.K. Prajapati, M.C. Varia, *Liq. Cryst.* 40 (2013) 1151–1158.
- [11] (a) G. Dantlgraber, S. Diele, C. Tschierske, *Chem. Commun.* (2002) 2768–2769;
(b) C.V. Yelamaggad, S.K. Prasad, G.G. Nair, I.S. Shashikala, D.S.S. Rao, C.V. Lobo, S. Chandrasekhar, *Angew. Chem. Int. Ed.* 43 (2004) 3429–3432;
(c) M. Horčić, J. Svoboda, V. Novotná, D. Pocięchac, E. Gorecka, *RSC Adv.* 8 (2018) 22974–22985.
- [12] N.W. Adams, J.S. Bradshaw, J.-M. Bayona, K.E. Markides, M.L. Lee, *Mol. Cryst. Liq. Cryst.* 147 (1987) 43–60.
- [13] H. Steinfink, B. Post, I. Fankuchen, *Acta Crystallogr.* 8 (1955) 420–424.
- [14] Y. Naito, R. Ishige, M. Itoh, M. Tokita, J. Watanabe, *Chem. Lett.* 37 (2008) 880–881.
- [15] J. Yang, D. Huang, F. Ding, K. Zhao, W. Guan, L. Zhang, *Mol. Cryst. Liq. Cryst.* 281 (1996) 51–56.
- [16] C. Keith, R.A. Reddy, A. Hauser, U. Baumeister, C. Tschierske, *J. Am. Chem. Soc.* 128 (2006) 3051–3066.
- [17] T. Itahara, S. Furukawa, K. Kubota, M. Morimoto, M. Sunose, *Liq. Cryst.* 40 (2013) 589–598.
- [18] A. Yoshizawa, *Liq. Cryst.* 44 (2017) 1877–1893 (and references cited therein).